This article has been accepted for publication in a future issue of this journal, but has not been fully edited. Content may change prior to final publication. Citation information: DOI 10.1109/TAP.2015.2444420, IEEE Transactions on Antennas and Propagation

Square Loop and Slot Frequency Selective Surfaces Study for Equivalent Circuit Model Optimization

David Ferreira, *Student Member, IEEE,* Rafael F. S. Caldeirinha, *Member, IEEE,* Iñigo Cuiñas, *Senior Member, IEEE,* and Telmo R. Fernandes, *Member, IEEE*

***Abstract*—This paper presents a parametric study of square loop and square slot frequency selective surfaces (FSS) aimed at their equivalent circuit (EC) model optimization. Consideration was given to their physical attributes, *i.e.* the unit cell dimensions and spacing, substrate thickness and dielectric properties, for several frequencies and plane wave incident angles. Correlation analysis and evaluation of the influence of physical related input parameters on the FSS performance, is presented. Subsequent optimization factor for the square loop classical EC model is analyzed, and a novel EC model formulation for the square slot FSS, is proposed. The performance of the proposed EC model was assessed against results obtained from appropriate electromagnetic (EM) simulations, based on a root-mean-square error (RMSE) criteria. Results demonstrate the validity of the optimized EC model, in which good estimations of the frequency response of FSS structures were obtained. Significant reduction of the resonant frequency offsets, in the order of 650 (from 910 to 260) and 460 (770 to 310) MHz, were obtained for square loops and square slots, respectively. The models were further validated against measurements performed on two physical FSS prototypes inside an anechoic chamber, at 2.4 GHz. Relatively good agreement was obtained between measurements of real FSS prototypes and results obtained with the EC model. Finally, this work is sought to provide the necessary refinement of elementary models for further studies with more complex and novel FSS structures.**

***Index Terms*—Frequency selective surfaces (FSS), equivalent circuits, indoor radio communication, radio propagation, simulation, measurement.**

I. Introduction

In recent years, the world has witnessed a significant increase in wireless devices operating at various frequencies across the usable spectrum range [1]. However, in some locations, blocking the usage of some devices in favor of others may be advantageous. In office buildings, a company may desire to block mobile phone coverage, while allowing the availability of its internal Wi-Fi system. In residential urban environments, one user may want to minimize the co-channel interference from neighbor Wi-Fi systems [1, 2].

Proposals for blocking radio waves arose for different applications, but most of them seem to not discriminate between desired and undesired frequencies, attenuating both: metallic shielding, reinforced concrete walls, and even soft barriers are among these solutions. Frequency selective surfaces (FSS) can therefore perform an important role in this topic, contributing to interference mitigation and wireless security in indoor radio environments. Although FSS are envisaged to selectively confine radio propagation in indoor areas, by artificially increasing the radio transmission loss naturally caused by building walls [3, 4], it may also be applied to other areas of interest, such as radomes [5, 6], dichroic filters [2] or artificial beam steering [7, 10].

While FSS applications have been growing exponentially, their analysis techniques are less developed. This paper contributes to the current open literature by improving on the existing equivalent circuit (EC) equations for the elementary square loop (or square ring) and square slot FSS. In addition, it provides the researchers with further insight into these structures, which will prove to be useful for subsequent work, including more complex and novel FSS structures.

Sections II and III present the square loop and square slot FSS designs, as well as their EC representation. Section IV introduces the proposed empirical optimization for the EC equations, with simulation results and estimation error assessment. A practical validation of the proposed equations is shown in sections V to VII, with description of the prototype simulations, measurement setup and results. All this effort is expected to be useful for further studies with more complex structures. Finally, in section VIII, the main conclusions are presented.

II. Square Loop FSS design

The square loop FSS is a canonical design when it comes to understanding the behavior of this type of structures. These present a band reject frequency response, which depends on the physical dimensions. Its relatively simple shape makes it ideal to build a prototype for performance assessment. Fig. 1a) presents a square loop structure.

The equivalent circuit model offers a simple and fast method in FSS analysis, which stands as a good alternative to full wave simulations. The transmission line analogy supports this model, in which equivalent inductive (L) and capacitive (C) lumped components construct the FSS. The quasi-static EC approximation of conducting strips developed by *Markuvitz* [11] allows the computation of the values for L and C. Fig. 1b) shows the EC model used for the square loop FSS. For Transverse Electrical (TE) wave incidence, the vertical strips

David Ferreira is with the Instituto de Telecomunicações, Leiria, Portugal. He is also with the University of Vigo, Dept. Teoría do Sinal e Comunicacións, Vigo, Spain.

Rafael. F. S. Caldeirinha and Telmo R. Fernandes are with the Instituto de Telecomunicações, Leiria, Portugal and Polytechnic Institute of Leiria, School of Technology and Management, Leiria, Portugal. They are also with the University of South Wales, School of Engineering, Treforest, United Kingdom (e-mail: rafael.caldeirinha@ipleiria.pt).

Iñigo Cuiñas is with the Universidade de Vigo, Dept. Teoría do Sinal e Comunicacións, Vigo, Spain.

This article has been accepted for publication in a future issue of this journal, but has not been fully edited. Content may change prior to final publication. Citation information: DOI 10.1109/TAP.2015.2444420, IEEE Transactions on Antennas and Propagation

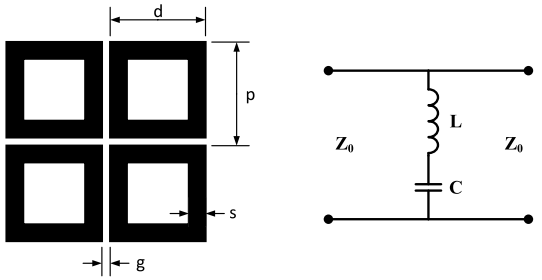

(a) (b)

Fig. 1: Square Loop: a) FSS design; b) EC model.

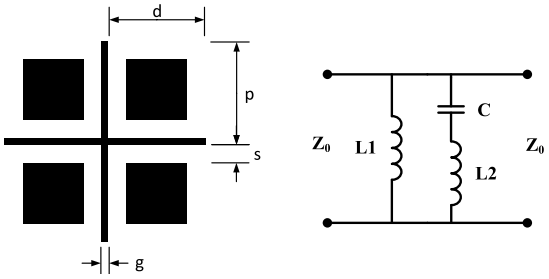

(a) (b)

Fig. 2: Square Slot: a) FSS design; b) EC model.

act as an inductive impedance in the equivalent circuit, and the horizontal gratings as a capacitive impedance.

Both L and C values of the EC are commonly calculated using equations (1) and (2), where d, p, s and g are the dimensions of the square loop of Fig. 1a) and θ is the incidence angle in relation to the normal incidence. The p and w parameters in equations (3) to (6) should be replaced by the appropriate inputs depicted in equations (1) and (2) [11–14].

$$\frac{X_L}{Z_0} = \omega L = \frac{d}{p}\cos\theta \; F(p, 2s, \lambda, \theta), \tag{1}$$

$$\frac{B_C}{Y_0} = \omega C = 4\frac{d}{p}\sec\theta \; F(p, g, \lambda, \theta)\varepsilon_{eff}, \tag{2}$$

where,

$$F(p, w, \lambda, \theta) = \frac{p}{\lambda}\left[\ln\left(\csc\frac{\pi w}{2p}\right) + G(p, w, \lambda, \theta)\right] \tag{3}$$

$$G(p, w, \lambda, \theta) = \frac{1}{2}\times \\ \times \frac{(1-\beta^2)^2\left[\left(1-\frac{\beta^2}{4}\right)(A_+ + A_-) + 4\beta^2 A_+ A_-\right]}{\left(1-\frac{\beta^2}{4}\right) + \beta^2\left(1+\frac{\beta^2}{2}-\frac{\beta^4}{8}\right)(A_+ + A_-) + 2\beta^6 A_+ A_-} \tag{4}$$

with,

$$A_\pm = \frac{1}{\sqrt{\left[1 \pm \frac{2p\sin\theta}{\lambda} - \left(\frac{p\cos\theta}{\lambda}\right)^2\right]}} - 1 \tag{5}$$

$$\beta = \sin\left(\frac{\pi w}{2p}\right) \tag{6}$$

The factor ε_{eff} in equation (2) was not present in previous publications, however it was introduced by [2] with the value $\varepsilon_{eff} = 0.5\,(\varepsilon_r + 1)$ and used for square loop FSS in [14] . This parameter represents an effective value to adjust the dielectric permittivity. Nevertheless, it was found through several simulations that the presence or absence of this adjustment factor is only accurate for situations where the dielectric substrate is either very thick ($> \lambda/5$), or is very thin ($< \lambda/100$), respectively. The EC equations based on [11] have limitations regarding their validity, such as: $w/p \ll 1$, $p/\lambda \ll 1$ and $p(1+\sin\theta)/\lambda < 1$. Nonetheless, such equations may lead to inaccurate results depending on substrate size and properties, even meeting these conditions.

Assuming an FSS with dimensions: $d = 20$ mm, $s = 5$ mm and $g = 2$ mm, equations (1) and (2), (excluding the ε_{eff} parameter) result in a resonance frequency of 7.39 GHz. Alternatively using ε_{eff} for a FR4 substrate ($\varepsilon_r = 4.4$), a resonant frequency of 4.82 GHz is obtained. This is a substantial difference despite of the substrate thickness, and as such, it undermines the EC simulation results.

III. Square Slot FSS design

Unlike its counterpart, the square slot FSS frequency response is band pass, also depending on its physical dimensions. Regarding its shape, this design is interpreting as the geometrical opposite of the square loop variant, since the conducting and non-conducting regions are reversed, as illustrated in Fig. 2.

Authors in [15] rely on the same equations utilized in the square loop case in order to calculate both L and C values of the EC circuit (which instead of being a series LC as in the square loop, for the square slot it is a parallel LC) and use the dimensions presented in Fig. 2a. Other authors, such as [16] and [17], use a simplified version of those equations, while [18] and [19] apply curve fitting to find the L and C values. However, it was found the EC depicted in Fig. 2b yields better frequency response curves. Equations (7) to (12) have been obtained for this square slot EC circuit.

$$\frac{X_{L1}}{Z_0} = \omega L1 = \cos\theta \; F(p, g, \lambda, \theta), \tag{7}$$

$$\frac{X_{L2int}}{Z_0} = \frac{p-2s}{p}\cos\theta \; F(p, d-2s, \lambda, \theta), \tag{8}$$

$$\frac{X_{L2}}{Z_0} = \omega L2 = \frac{X_{L2int}}{Z_0} + \frac{s}{d-2s+g}\frac{X_{L1}}{Z_0}, \tag{9}$$

$$\frac{B_{C1}}{Y_0} = 4\sec\theta \; F(p, d, \lambda, \theta), \tag{10}$$

$$\frac{B_{C2}}{Y_0} = 4\sec\theta \; F(d-s, s, \lambda, \theta), \tag{11}$$

$$\frac{B_C}{Y_0} = \omega C = \left(1.75\frac{B_{C1}}{Y_0} + 0.6\frac{B_{C2}}{Y_0}\right)\varepsilon_{eff}, \tag{12}$$

This article has been accepted for publication in a future issue of this journal, but has not been fully edited. Content may change prior to final publication. Citation information: DOI 10.1109/TAP.2015.2444420, IEEE Transactions on Antennas and Propagation

TABLE I: EM simulation parameters

	Parameter	Value Range
Substrate	Relative permittivity	$[1.1, 8]$
	Thickness	$[0.1, 20]$ mm
FSS	d	$[12, 32]$ mm
	s, with $(2s < d)$	$[0.5, 12]$ mm
	g	$[1, 6]$ mm

The limits of validity of this new set of equations are considered to be equal to the limits of equations (1) to (6) provided by [11]. In equation (7), X_{L1} represents the inductance of the lines with g width. X_{L2} in (8) represents the inductance of the inner squares (with $d - 2s$ sides) with the lines with g width, multiplied by a scaling factor defined by $\frac{p-2s}{p}$ which represents the s length discontinuities. This X_{L2} is however influenced by X_{L1}, with a relation depicted in (9).

The capacitance value is obtained from two intermediate calculations. Equation (10) depicts the equivalent capacitor between the parallel lines with g thickness (and length d). Equation (11) represents the capacitor between the inner square and the g thickness lines. Finally, in equation (12), the overall value is calculated using the obtained and depicted relation.

Regarding the ε_{eff} value present in (12), this is to be replaced with a new parameter, shown in the next section of the paper.

IV. Proposed EC model optimizations

A. Parametric simulations

By performing a wide set of parametric simulations, using the Electromagnetic (EM) simulation software CST Microwave Studio, empirical equations for the ε_{eff} parameter were achieved for both square loop and square slot FSS, yielding to lower errors when compared to the classical set of equations. A wide range of parameters were considered in the simulations, such as the substrate thickness and its permittivity value, as well as the specific dimensions of the FSS unit cells defined by the d, p, s and g values. Table I presents value ranges of the parameters, which results in FSS with resonance frequency from 1 up to 15 GHz.

B. Parameters' influence on FSS frequency response

With the EM simulations covering the aforementioned range, a few conclusions were drawn regarding the parameters influence on the resonance frequency of the FSS. These observations assisted in the development of the empirical EC equations.

Both the substrate thickness and relative permittivity exhibited an impact on the resonance frequency. Fig. 3 shows the evolution of the square loop and square slot resonance frequencies versus the substrate thickness, for different substrate permittivity values. As can be seen in the square loop case, with $\varepsilon_r = 4.4$ and $\varepsilon_r = 2.2$, both curves follow the same profile, albeit with smaller range in the latter.

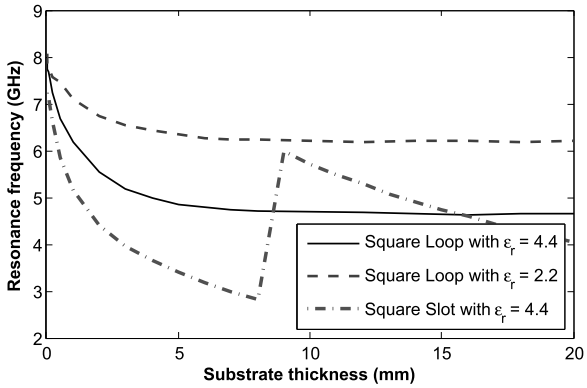

Fig. 3: Substrate influence on square loop FSS with $\varepsilon_r = 4.4$ and $\varepsilon_r = 2.2$, and on square slot FSS with $\varepsilon_r = 4.4$, both with unit cell dimensions $d = 20$mm, $s = 5$mm and $g = 4$mm.

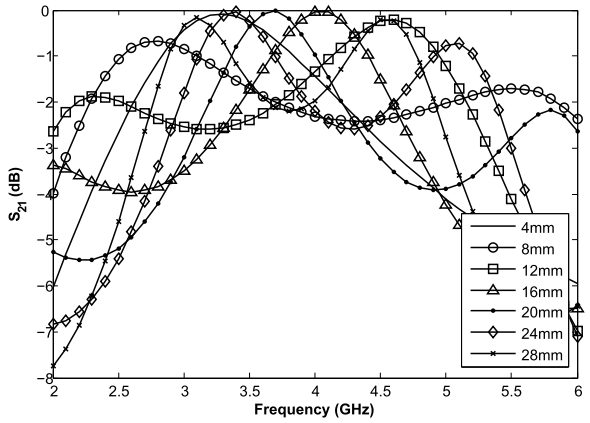

Fig. 4: Frequency response for a square slot with dimensions $d = 16$mm, $s = 2$mm and $g = 4$mm and substrate permittivity $\varepsilon_r = 4.4$ in relation to the increase in substrate thickness.

On the other hand, the square slot FSS yielded a different behavior when varying the substrate thickness. Contrary to the square loop FSS, the resonant frequency seems to not stabilize for increasing substrate thicknesses, as can be seen in Fig. 4. This behavior is influenced by the substrate permittivity value (it does not occur for $\varepsilon_r = 1$), and also by its thickness. From observations, these multiple resonances are due to the EM wave propagation speed inside the substrate (which depends on the permittivity). The higher and lower sections of such observed frequency behavior are dependent on whether the electric fields at the medium transition are at the peak or minimum values, respectively. Recalling Fig. 3, the plotted transition in resonance frequency for the square slot case, was at a substrate thickness value where the higher resonance frequency had better S_{21} than the lower resonance frequency. Such observed phenomena may be useful in specific applications, where a dual or higher band pass property, without the need to employ more complex FSS structures, is required.

Regarding FSS specific unit cell dimensions, by changing parameters d, s and g values yields different frequency responses. By modifying the d parameter only, significant

This article has been accepted for publication in a future issue of this journal, but has not been fully edited. Content may change prior to final publication. Citation information: DOI 10.1109/TAP.2015.2444420, IEEE Transactions on Antennas and Propagation

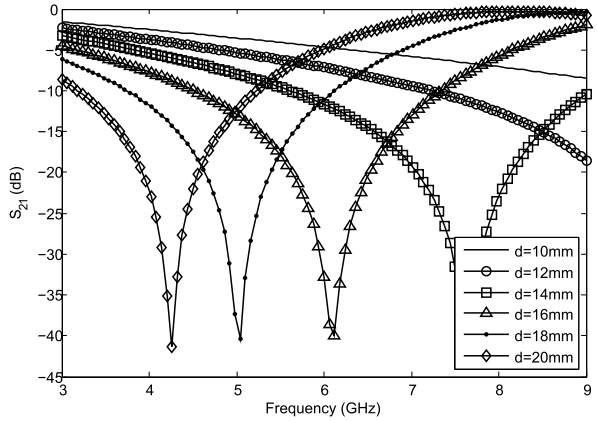

Fig. 5: Influence of d parameter on a square loop FSS frequency response, with dimensions $s = 3$mm, $g = 4$mm, substrate permittivity $\varepsilon_r = 4.4$ and 1.5mm in thickness.

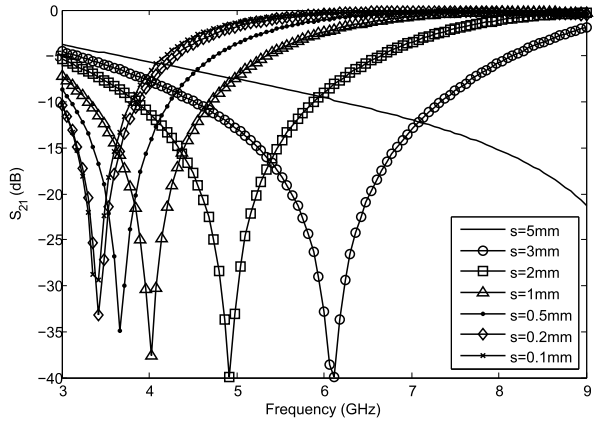

Fig. 6: Influence of s parameter on a square loop FSS frequency response, with dimensions $d = 16$mm, $g = 4$mm, substrate permittivity $\varepsilon_r = 4.4$ and 1.5mm in thickness.

changes are visible in the resonance frequency, as depicted in Fig. 5. On the other hand, by varying the s value alone, it also results in significant change in the resonance frequency, but mostly the bandwidth of the FSS. By decreasing s, the bandwidth becomes narrower, as it can be seen in Fig. 6. With a proper adjustment of both d and s dimensions, a steady resonance frequency can be found while also adjusting for the desired bandwidth. Besides, if kept with a small value, the g parameter will make the FSS resonance frequency less sensible to incoming radio wave incidence angle, as exhibited by Fig. 7.

C. Square Loop proposed EC equation correction factor

The proposed improvement to the classical EC equations consists of an empirical equation to replace the ε_{eff} parameter used by [14]. Equation (13) introduces this concept.

ε_{Corr} depends on the square loop dimensions (p, s and g), the substrate thickness (h) and the substrate relative permittivity (ε_r). This equation is valid for, at least, the EM simulation

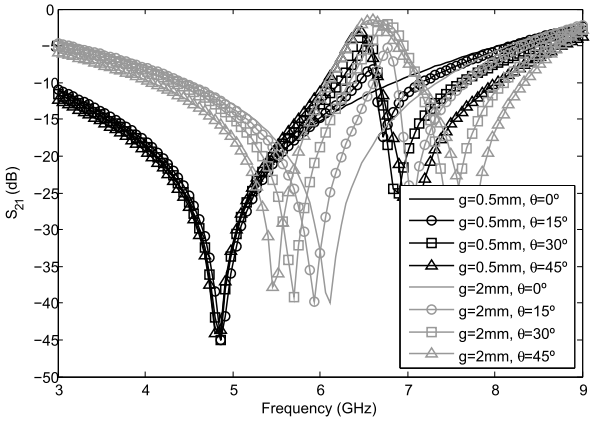

Fig. 7: Influence of g parameter on a square loop FSS frequency response, with dimensions $d = 16$mm, $s = 3$mm, substrate permittivity $\varepsilon_r = 4.4$ and 1.5mm in thickness.

parametric range specified in Table I. Since this correction factor is applied to the base equations depicted in section II, the same normalized limits of validity should also be applied. It must be noted, however, that for some instances of parameter combinations from Table I, the limits of validity provided by [11] are not entirely obeyed, and as such, the EC model may have an increased deviation from EM simulations.

$$\varepsilon_{Corr} = \frac{\varepsilon_r + 1}{2} - \frac{\varepsilon_r - 1}{2} \times \times \exp\left(\frac{-13h}{p}\right) - \left(\frac{100s^2}{d} - 2g + 10h\right) \mathrm{m}^{-1} \quad (13)$$

Table II presents a comparison between the full wave simulation and the EC formulation with ε_{eff} and ε_{Corr} factors for different FSS unit cell sizes, substrate thickness and permittivity values. A more extensive analysis, with results obtained for both normal and 45° incidences are shown. In a worst-case scenario, the prediction errors were substantially reduced in all cases. It should be noted some examples shown in the table fall near, or even outside, of the normalized limits of validity specified in section II. This fact brings an inevitable increase in error values from both the classical and the proposed equations, albeit the latter still producing better estimations. Furthermore, two examples which are outside of the initial parametric range were also included to further assess the EC equations. The ε_{Corr} parameter when applied to (2), provides better approximations between full wave simulations and the EC model, when compared to the original EC model without this correction factor, or with the ε_{eff} value shown in [14].

Table III provides the root mean square error (RMSE) for the complete parametric simulation, in which the resonance frequencies of the EC simulations were evaluated against the EM results. A value of 260 MHz was achieved with the proposed ε_{Corr} correction factor, which is considerably better than the 910 MHz obtained by using only the ε_{eff} correction factor. However, it should be noted that during the EM simulations, and for the 45° oblique incidence cases,

This article has been accepted for publication in a future issue of this journal, but has not been fully edited. Content may change prior to final publication. Citation information: DOI 10.1109/TAP.2015.2444420, IEEE Transactions on Antennas and Propagation

TABLE II: Simulation results for square loop FSS

FSS properties (mm)	Simulation tool	Frequency (GHz) for incidence angle theta		Error compared to EM for incidence angle theta	
		0°	45°	0°	45°
$\varepsilon_r = 4.4$ $h = 1$ $d = 16$ $s = 2$ $g = 2$	EM	**4.67**	**4.58**	-	-
	Classic EC	6.49	6.16	39%	34.5%
	EC with ε_{eff}	4.08	4.01	-12.6%	-12.4%
	EC with ε_{Corr}	**4.90**	**4.77**	**4.9%**	**4.1%**
$\varepsilon_r = 4.4$ $h = 1$ $d = 16$ $s = 3$ $g = 2$	EM	**6.10**	**5.51**	-	-
	Classic EC	8.43	7.27	38.2%	31.9%
	EC with ε_{eff}	5.60	4.90	-8.2%	-11.1%
	EC with ε_{Corr}	**6.03**	**5.81**	**-1.1%**	**5.4%**
$\varepsilon_r = 4.4$ $h = 1$ $d = 20$ $s = 4$ $g = 2$	EM	**4.93**	**4.61**	-	-
	Classic EC	6.32	5.93	28.2%	28.6%
	EC with ε_{eff}	4.04	3.96	-18.1%	-14.1%
	EC with ε_{Corr}	**5.05**	**4.87**	**2.4%**	**5.6%**
$\varepsilon_r = 4.4$ $h = 1$ $d = 24$ $s = 4$ $g = 4$	EM	**4.00**	**3.77**	-	-
	Classic EC	5.10	4.69	27.5%	24.4%
	EC with ε_{eff}	3.28	3.19	-18%	-15.4%
	EC with ε_{Corr}	**4.21**	**4.00**	**5.3%**	**6.1%**
$\varepsilon_r = 2.2$ $h = 0.127$ $d = 5$ $s = 0.25$ $g = 0.5$	EM	**14.2**	**14.5**	-	-
	Classic EC	15.1	14.8	6.3%	2.1%
	EC with ε_{eff}	12.0	11.9	-15.5%	-17.9%
	EC with ε_{Corr}	**14.1**	**13.8**	**-0.7%**	**-4.8%**
$\varepsilon_r = 2.2$ $h = 0.254$ $d = 18$ $s = 1$ $g = 5$	EM	**4.96**	**4.76**	-	-
	Classic EC	5.34	5.04	7.7%	5.9%
	EC with ε_{eff}	4.31	4.16	-13.1%	-12.6%
	EC with ε_{Corr}	**5.15**	**4.89**	**3.8%**	**2.7%**
$\varepsilon_r = 6.15$ $h = 1.9$ $d = 70$ $s = 14$ $g = 10$	EM	**1.54**	**1.36**	-	-
	Classic EC	1.88	1.73	22.1%	27.2%
	EC with ε_{eff}	1.07	1.05	-30.5%	-22.8%
	EC with ε_{Corr}	**1.63**	**1.54**	**5.8%**	**13.2%**
$\varepsilon_r = 6.15$ $h = 2.5$ $d = 32$ $s = 8$ $g = 2$	EM	**2.96**	**2.62**	-	-
	Classic EC	4.44	4.19	50%	59.9%
	EC with ε_{eff}	2.49	2.47	15.9%	5.7%
	EC with ε_{Corr}	**3.03**	**2.98**	**2.4%**	**13.7%**

TABLE III: RMSE for square loop FSS EC equation

Simulation tool	RMSE vs EM
Classic EC	1.20 GHz
Classic EC with ε_{eff}	0.91 GHz
Classic EC with ε_{Corr}	0.26 GHz

multiple resonance points were visible at higher frequencies. However, only the lowest resonance point was considered for this analysis.

D. Square Slot proposed EC equation correction factor

Observing the curves presented in Figs. 3 and 4, one concludes that the behavior of square slot FSS differs from the square loop variant, more specifically, the resonant frequency for low substrate thickness is different, and the response differs considerably as thickness increases. To predict this behavior through equivalent circuit, different and novel equations were devised and presented in section III. Furthermore, similar to the square loop case, these equations are not influenced by substrate thickness and permittivity. As such, an empirical equation different to the one in IV-C, is proposed for the square slot FSS.

$$\varepsilon_{Corr} = \frac{\varepsilon_r + 1}{2} - \frac{\varepsilon_r - 1}{2} \exp\left(-955 h \mathrm{m}^{-1}\right) - \left(\frac{155 s^2}{d}\right) \mathrm{m}^{-1} \tag{14}$$

Equation (14) has some similarities to (13), including the limits of validity, but adjusted for the square slot FSS case. Also, and due to the behavior observed in Figs. 3 and 4, this equation is only valid for FSS unit cells with the substrate thickness smaller than approximately $d - 2s$, which is when two frequencies of resonance are present and with identical S_{21} values.

Table IV presents some simulation results for square slot FSS with different unit cell dimensions, substrate thickness and permittivity values. From a close inspection of the depicted results, the proposed EC equations and ε_{Corr} for square slot FSS yields better estimates than both classic EC equations and classic EC with ε_{eff} factor. Similarly to the cases in Table II, some examples in Table IV are also near, or even outside, of the normalized limits of validity specified in section III, which brings an inevitable increase in error values. Also, the two simulation cases outside of the parametric range used in Table II were also included. Table V provides the RMSE of the overall parametric EC simulations.

V. Prototype Design and Simulations

In order to validate the previously proposed EC equations, two FSS physical prototypes were built and measured in a controlled environment. However, before this step, the dimensions of the unit cell for those prototypes were selected.

In total, two walls were prepared for simulation and construction: one band reject and one band pass, at a center frequency of 2.4 GHz. Table VI depicts the chosen dimensions for the FSS and their corresponding resonance frequencies for two incidence angles.

The FSS prototypes were planned with a small s dimension. In section IV it was shown that smaller values of s yield narrower frequency bandwidths. So, the goal of these prototypes was twofold: to confirm if the actual frequency bandwidth was similar to the simulated one; and to assess if the chosen narrow conducting lines were achievable with the in-house PCB production setup. Section VII provides plots with the frequency response of the prototypes.

VI. Measurement Setup

To evaluate the simulation results, the FSS prototypes were etched in a 51 by 50 cm FR4 substrate with 1.5 mm in thickness and $\varepsilon_r = 4.4$. Fig. 8 shows the prototypes.

In order to properly accommodating the FSS inside the anechoic chamber, a support structure was developed. The structure measures 1.8×2 m ($h \times w$) and it was covered on one side with pyramidal RF absorbents and with aluminum foil. With this structure, diffraction contamination of the results is

This article has been accepted for publication in a future issue of this journal, but has not been fully edited. Content may change prior to final publication. Citation information: DOI 10.1109/TAP.2015.2444420, IEEE Transactions on Antennas and Propagation

TABLE IV: Simulation results for square slot FSS

FSS properties (mm)	Simulation tool	Frequency (GHz) for incidence angle theta		Error compared to EM for incidence angle theta	
		0°	45°	0°	45°
$\varepsilon_r = 4.4$ $h = 1$ $d = 16$ $s = 2$ $g = 2$	EM	**4.32**	**4.34**	-	-
	Classic EC	6.49	6.16	50.2%	41.9%
	EC with ε_{eff}	4.08	4.01	-5.6%	-7.6%
	EC with ε_{Corr}	**4.66**	**4.58**	**7.9%**	**5.5%**
$\varepsilon_r = 4.4$ $h = 1$ $d = 16$ $s = 3$ $g = 2$	EM	**5.18**	**5.14**	-	-
	Classic EC	8.43	7.27	62.7%	41.4%
	EC with ε_{eff}	5.60	4.90	8.1%	-4.7%
	EC with ε_{Corr}	**5.47**	**5.34**	**5.6%**	**3.9%**
$\varepsilon_r = 4.4$ $h = 1$ $d = 20$ $s = 4$ $g = 2$	EM	**4.40**	**4.38**	-	-
	Classic EC	6.32	5.93	43.6%	35.4%
	EC with ε_{eff}	4.04	3.96	-8.2%	-9.6%
	EC with ε_{Corr}	**4.43**	**4.33**	**0.7%**	**-1.1%**
$\varepsilon_r = 4.4$ $h = 1$ $d = 24$ $s = 4$ $g = 4$	EM	**3.59**	**3.58**	-	-
	Classic EC	5.10	4.69	42.1%	31.0%
	EC with ε_{eff}	3.28	3.19	-8.6%	-10.9%
	EC with ε_{Corr}	**3.59**	**3.50**	**0%**	**-2.2%**
$\varepsilon_r = 2.2$ $h = 0.127$ $d = 5$ $s = 0.25$ $g = 0.5$	EM	**14.1**	**14.4**	-	-
	Classic EC	15.1	14.8	7.1%	2.8%
	EC with ε_{eff}	12.0	11.9	-14.9%	-17.4%
	EC with ε_{Corr}	**15.7**	**15.4**	**11.3%**	**6.9%**
$\varepsilon_r = 2.2$ $h = 0.254$ $d = 18$ $s = 1$ $g = 5$	EM	**4.62**	**4.60**	-	-
	Classic EC	5.34	5.04	15.6%	9.6%
	EC with ε_{eff}	4.31	4.16	-6.7%	-9.6%
	EC with ε_{Corr}	**4.93**	**4.78**	**6.7%**	**3.9%**
$\varepsilon_r = 6.15$ $h = 1.9$ $d = 70$ $s = 14$ $g = 10$	EM	**1.28**	**1.30**	-	-
	Classic EC	1.88	1.73	46.9%	33.1%
	EC with ε_{eff}	1.07	1.05	-16.4%	-19.2%
	EC with ε_{Corr}	**1.12**	**1.10**	**-12.5%**	**-15.4%**
$\varepsilon_r = 6.15$ $h = 2.5$ $d = 32$ $s = 8$ $g = 2$	EM	**2.34**	**2.34**	-	-
	Classic EC	4.44	4.19	89.7%	79.1%
	EC with ε_{eff}	2.49	2.47	6.4%	5.6%
	EC with ε_{Corr}	**2.38**	**2.35**	**1.7%**	**0.4%**

TABLE V: RMSE for square slot FSS EC equation

Simulation tool	RMSE vs EM
Classic EC	1.46 GHz
Classic EC with ε_{eff}	0.77 GHz
Proposed EC with ε_{Corr}	0.31 GHz

minimized, and the transmission mainly occurs in the square center window, which measures 48×48 cm.

On the perpendicular measurement setup, both transmitter and receiver sides were connected to two identical low profile ultra wide band antennas. The antennas have an omnidirectional pattern in the azimuth plane.

The oblique incidence measurements consisted in placing both transmitter and receiver supports at an angle of $45°$. Distance from both antennas to the center of the structure was 1.05 m.

The frequency response of the prototype was assessed using a Vector Network Analyzer (VNA) directly connected to both

TABLE VI: FSS dimensions and resonance frequency

FSS type	Unit cell dimensions (mm)	EC resonance frequency (GHz) for incidence angle theta		EM resonance frequency (GHz) for incidence angle theta	
		0°	45°	0°	45°
Band reject	$d = 20$, $s = 0.5$, $p = 22$, $g = 2$	2.33	2.32	2.43	2.44
Band pass	$d = 20.5$, $s = 0.5$, $p = 22.5$, $g = 2$	2.32	2.31	2.41	2.43

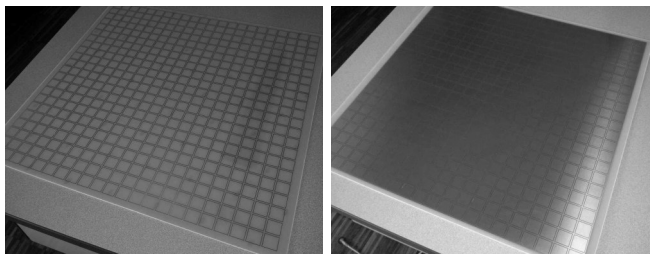

(a) (b)

Fig. 8: FSS prototypes: a) Square Loop; b) Square Slot.

transmitter and receiver antennas. Two measurements were performed with the above mentioned setup. Measurements featuring the unobstructed window, from this point forward designated as free-space (FS) measurement; and one with the FSS under test were carried out. Fig. 9 shows a block diagram of the overall measurement setup.

VII. Measurement Results

With the measurement setup defined and assembled, all the necessary measurements were performed in the anechoic chamber.

In Fig. 10, the measurement setup performance is shown. Observing the band reject FSS curve, one can extrapolate that the measurement setup is not free from contaminations, as the S_{21} value in the vicinity of the resonance frequency shows an irregular (and unpredicted) behavior. This fact is more visible in the oblique measurements mentioned later.

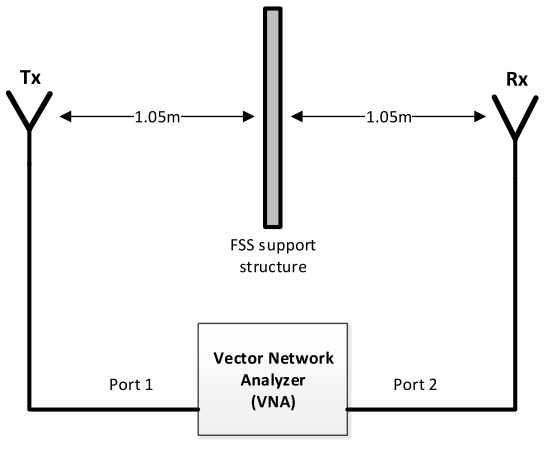

Fig. 9: Measurement setup block diagram.

This article has been accepted for publication in a future issue of this journal, but has not been fully edited. Content may change prior to final publication. Citation information: DOI 10.1109/TAP.2015.2444420, IEEE Transactions on Antennas and Propagation

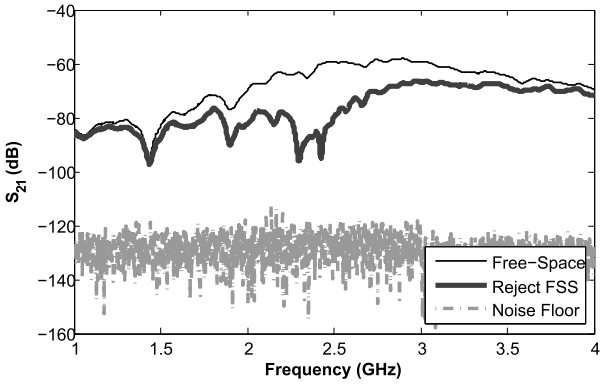

Fig. 10: Reference measurements perpendicular setup.

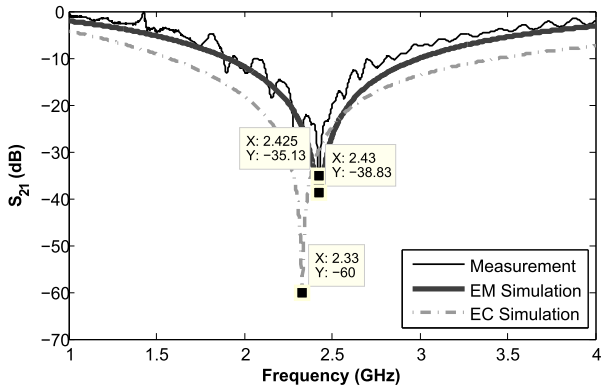

Fig. 11: Band reject FSS perpendicular measurement and EM simulation results.

Figs. 11 and 12 present the reject and band pass FSS results, respectively. In both cases, the EC simulation yielded similar results to those of both EM and measured results.

Regarding the oblique measurements, Figs. 13 and 14 depict those results. Viewing Fig. 13, one can undoubtedly confirm the presence of contamination in the measurement setup. This contamination of the results may be due to diffraction, as well as reflection over the anechoic chamber walls, which are metallic backed, since the RF absorbents are on the lower limit of their usable frequency range. Despite this, both reject and band pass FSS show relatively good agreement with the EM simulation results. Table VII summarizes both simulation and measurement results for the FSS prototypes.

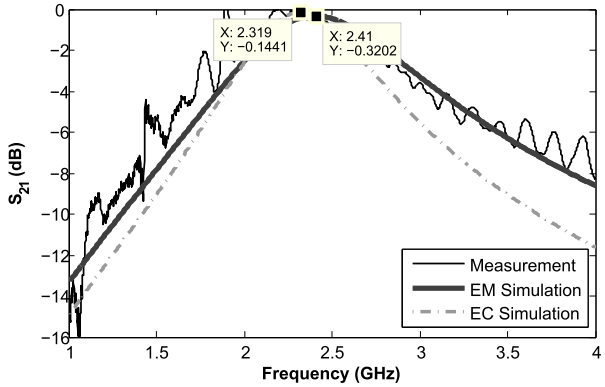

Fig. 12: Band pass FSS perpendicular measurement and EM simulation results.

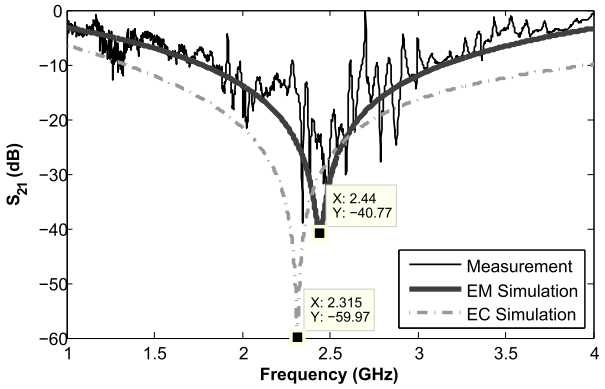

Fig. 13: Band reject FSS oblique measurement and EM simulation results.

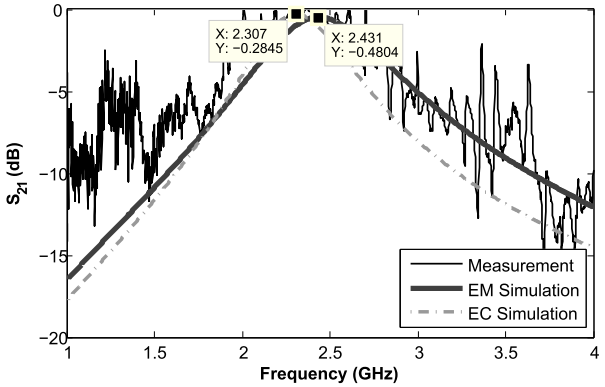

Fig. 14: Band pass FSS oblique measurement and EM simulation results.

VIII. Conclusions

This paper proposes novel contributions to the EC equations, traditionally used to model square loop and square slot

TABLE VII: FSS simulation and measurement results

Type of results	Band reject FSS frequency (GHz) for incidence angle theta		Band pass FSS frequency (GHz) for incidence angle theta	
	0°	45°	0°	45°
Classic EC	3.26	3.22	3.15	3.11
EC with ε_{eff}	2.00	1.99	1.93	1.93
EC with ε_{Corr}	2.33	2.32	2.32	2.31
EM	2.43	2.44	2.41	2.43
Measurement	2.43	2.48	2.28	2.36

FSS, in order to improve their accuracy for actual designs. For the square slot FSS case, novel EC equations intended to better represent the frequency response, are proposed. An extensive set of EM parametric simulations using the CST Microwave Studio software were initially used to define and adjust the new parameters, covering FSS resonance frequencies, ranging from 1 up to 15 GHz.

The empirical manipulation to the classical square loop FSS EC equations was shown to provide relatively good estimates in terms of predicted resonance frequency, and thus minimizing the errors between EC and EM simulations. A calculated RMSE value of 260 MHz, which is considerably lower than that provided by the classical equations (1.2 GHz), or even with the simple ε_{eff} factor (910 MHz), was obtained.

The proposed equations and correction factor for the square slot, also provided relatively good results, albeit slightly worse than those from the square loop, yielding a calculated RMSE of 310 MHz, against the 820 MHz obtained with the classical formulations with the ε_{eff} factor. This EC with three lumped elements is observed to be the required minimum to appropriately describing the frequency response of such structure, both on the first band pass frequency, as well as the roll-off rate to the higher frequency first rejection band. Two simulations for each FSS variant with parameters outside of the initial parametric range were included in the results of Tables II and IV. Results show that both EC proposed equations still provide moderate to good results when compared to other EC equations.

Two FSS prototypes, with dimensions of 51 by 50 cm, have been used to validate the proposed model against measurements in an anechoic chamber. These prototypes performed relatively well within the simulated results, albeit some contamination due to diffraction in the measurements. These were etched to provide narrow bandwidths, although, due to mechanical constraints, one may need to use other methods in order to have much narrower bandwidths, such as multilayer FSS or addition of lumped elements.

In summary, this research study, coupled with the development and measurement of actual prototypes, highlights the benefits and limitations of lumped EC models, and the proposed formulas should be useful to determine a good first design for the target main resonance frequency using this type of FSS. Combined with full wave solvers, a good final design may be achieved within a reasonable time. Finally, this work should prove useful for further studies with more complex and novel structures, particularly at frequencies of interest within the 3G, 4G and 5G commercial bands.

ACKNOWLEDGMENT

The authors are grateful to Instituto de Telecomunicações Leiria, Portugal, to Polytechnic Institute of Leiria, School of Technology and Management, Portugal, and to Universidade de Vigo, Spain, for making available their facilities used in this research project. This research was partially supported by the Portuguese Government, Portuguese Foundation for Science and Technology, FCT, through the financial support provided under the QREN-POPH funding; and by the Spanish Government, Ministerio de Economía y Competitividad, Secretaría de Estado de Investigación, Desarrollo e Innovación, (project TEC2011-28789-C02-02), AtlantTIC Research Center and the European Regional Development Fund (ERDF).

REFERENCES

[1] M. Yang and A. K. Brown, "A Hybrid Model for Radio Wave Propagation Through Frequency Selective Structures (FSS)," IEEE Transactions On Antennas And Propagation, Vol. 58, No. 9, September 2010;

[2] B. A. Munk, "Frequency Selective Surfaces Theory and Design," Book, John Wiley & Sons, NY USA, 2000, ISBN 0-471-37047-9;

[3] M. Raspopoulos and S. Stavrou, "Frequency Selective Buildings Through Frequency Selective Surfaces," IEEE Transactions On Antennas And Propagation, Vol. 59, No. 8, August 2011;

[4] G. Kiani et al, "Cross-Dipole Bandpass Frequency Selective Surface for Energy-Saving Glass Used in Buildings," IEEE Transactions On Antennas And Propagation, Vol. 59, No. 2, February 2011;

[5] R. Nair and R. Jha, "Electromagnetic Design and Performance Analysis of Airborne Radomes: Trends and Perspectives," IEEE Antennas And Propagation Magazine, Vol. 56, No. 4, August 2014;

[6] H. Zhou et al, "Filter-Antenna Consisting of Conical FSS Radome and Monopole Antenna," IEEE Transactions On Antennas And Propagation, Vol. 60, No. 6, June 2012;

[7] T. Smith et al, "An FSS-Backed 20/30 GHz Circularly Polarized Reflectarray for a Shared Aperture L- and Ka-Band Satellite Communication Antenna," IEEE Transactions On Antennas And Propagation, Vol. 62, No. 2, February 2014;

[8] J. Shaker, R. Chaharmir and H. Legay, "Investigation of FSS-Backed Reflectarray Using Different Classes of Cell Elements," IEEE Transactions On Antennas And Propagation, Vol. 56, No. 12, December 2008;

[9] B. Liang et al, "Cylindrical Slot FSS Configuration for Beam-Switching Applications," IEEE Transactions On Antennas And Propagation, Vol. 63, No. 1, January 2015;

[10] I. Russo, L. Boccia, G. Amendola and G. Di Massa, "Tunable Pass-Band FSS for Beam Steering Applications," European Conference on Antennas and Propagation (EuCAP), April 2010;

[11] N. Marcuvitz, "Waveguide Handbook," New York, Peter Peregrinus Ltd., 1986, pp. 278-280;

[12] R. J. Langley and E. A. Parker, "EQUIVALENT CIRCUIT MODEL FOR ARRAYS OF SQUARE LOOPS," Electronic Letters, vol. 18, no. 7, pp. 294-296, April 1982;

[13] C. K. Lee and R. J. Langley, "Equivalent-circuit models for frequency-selective surfaces at oblique angles of incidence," IEE Proceedings, Vol. 132, no. 6, pp. 395-399, 1985;

[14] G. H. H. Sung et al, "A Frequency Selective Wall for Interference Reduction in Wireless Indoor Environments," IEEE Antennas and Propagation Magazine, vol. 48, no. 5, pp. 29-37, 2006;

[15] N. Qasem and R. Seager, "Indoor Band Pass Frequency Selective Wall Paper Equivalent Circuit & Ways to Enhance Wireless Signal," Loughborough Antennas & Propagation Conference (LAPC), November 2011;

[16] D. Wang, Y. Chang, W. Che and Y. Chow, "Miniaturized Dual-Band Loaded Frequency Selective Surface with Narrow Band Spacing," International Conference on Microwave and Millimeter Wave Technology (ICMMT), May 2012;

[17] K. Sarabandi and N. Behdad, "A Frequency Selective Surface With Miniaturized Elements," IEEE Transactions On Antennas And Propagation, Vol. 55, No. 5, May 2007;

[18] D. Wang, Y. Chang, W. Che and Y. Chow, "A novel low-profile tri-band frequency selective surface," IEEE Wireless Symposium, April 2013;

[19] M. Moallem, and K. Sarabandi, "A Single-layer Metamaterial-based Polarizer and Bandpass Frequency Selective Surface with an Adjacent Transmission Zero," IEEE International Symposium on Antennas and Propagation, July 2011.

David Ferreira (S'15) was born in Leiria, Portugal, in 1987. He received the Licenciatura and Master of Science degrees in Electrical and Electronics Engineering - Telecommunications branch, from the School of Technology and Management, Polytechnic Institute of Leiria, Leiria, Portugal, in 2008 and 2010, respectively.

He is a researcher at the Instituto de Telecomunicações, Leiria, Portugal. He is currently working toward the Ph.D. degree in electrical engineering at the University of Vigo, Spain, and his current research interests include radio wave propagation measurements, characterization and modeling.

Rafael F. S. Caldeirinha (M'00) was born in Leiria, Portugal, in 1974. He received the BEng (Hons) degree in Electronic and Communication Engineering from the University of Glamorgan, UK, in 1997. In 2001, he was awarded a Ph.D in Radiowave Propagation by the same University for his research work in vegetation studies at frequencies from 1 to 62.4 GHz.

He is currently Head of the Antennas & Propagation (A&P-Lr) research group at Instituto de Telecomunicações, Leiria, Portugal, and a Coordinator Professor in Mobile Communications at the School of Technology and Management (ESTG) of the Polytechnic Institute of Leiria (IPL), Portugal.

His research interests include studies of radiowave propagation through vegetation media, radio channel sounding and modeling and frequency selective surfaces, for applications at microwave and millimeter wave frequencies.

Prof. Caldeirinha has authored or co-authored more than 90 papers in conferences and international journals, 1 book chapter and 4 contributions to ITU-R Study Group which formed the basis of the ITU-R P.833-5 (2005) recommendation. He is a member of the editorial board of the International Journal of Communication Systems, IJCS (New York, Wiley), Program chair of WINSYS International Conference between 2006 and 2012, Appointed Officer for Awards and Recognitions of the IEEE Portugal section in 2014, and a Member of IEEE and IET.

Iñigo Cuiñas (M'08 SM'14) was born in Vigo, Spain, in 1971. He received his degree in Telecommunication Engineering in 1996, and his Ph.D. degree in 2000, both from the Universidade de Vigo, Spain.

He is currently Professor at the Dept. of Signal Theory and Communications, Universidade de Vigo. He is also Dean of the School of Telecommunication Engineering, where he teaches courses on Remote Sensing and Engineering to Society links.

His main research interest is focused on radio wave propagation in complex environments, as vegetation media; environmental aspects of radiofrequency systems, as the development of techniques to reduce the electromagnetic pollution; as well as to extend the use of radio technologies in rural and vegetation environments.

Prof. Cuiñas has authored or co-authored more than 55 papers in journals and 90 contributions to international conferences. He is also a reviewer of Proceedings of the IEEE, IEEE Transactions on Antennas and Propagation, IEEE Antennas and Wireless Propagation Letters, IEEE Antennas and Propagation Magazine, IEEE Transactions on Vehicular Technology, IEEE Transactions on Broadcasting, IEEE Communications Magazine, IET Microwaves, Antennas and Propagation, IET Communications, IET Sonar Radar and Navigation, and several international conferences.

Telmo R. Fernandes (S'05 M'06) received the Licenciatura degree in Electrical Engineering, Telecommunications and Electronics from the Sciences and Technology Faculty of the University of Coimbra, Portugal, in 1996 and the M.Sc. degree from the same University in 2000, for his study entitled "Channel Assignment on Cellular Networks using Neural Networks and Genetic Algorithms".

He was awarded the Ph.D. degree in Radiocommunication Systems by the University of Glamorgan, Glamorgan, UK, in 2007 for his research Programme in Radiowave Propagation through Vegetation. In 1997, he joined School of Technology and Management, Polytechnic Institute of Leiria, Leiria, where he is now a Senior Lecturer. He is currently a Researcher at the Instituto de Telecomunicações, Leiria, Portugal.